ORIGINAL PAPER

Ultraviolet polarisation sensitivity in the stomatopod crustacean *Odontodactylus scyllarus*

Sonja Kleinlogel · N. Justin Marshall

Abstract The ommatidia of crustacean eyes typically contain two classes of photoreceptors with orthogonally oriented microvilli. These receptors provide the basis for two-channel polarisation vision in the blue–green spectrum. The retinae of gonodactyloid stomatopod crustaceans possess a great variety of structural specialisations for elaborate polarisation vision. One type of specialisation is found in the small, distally placed R8 cells within the two most ventral rows of the mid-band. These ultraviolet-sensitive photoreceptors produce parallel microvilli, a feature suggestive for polarisation-sensitive photoreceptors. Here, we show by means of intracellular recordings combined with dye-injections that in the gonodactyloid species *Odontodactylus scyllarus*, the R8 cells of mid-band rows 5 and 6 are sensitive to linear polarised ultraviolet light. We show that mid-band row 5 R8 cells respond maximally to light with an *e*-vector oriented parallel to the mid-band, whereas mid-band row 6 R8 cells respond maximally to light with an e-vector oriented perpendicular to the mid-band. This orthogonal arrangement of ultraviolet-sensitive receptor cells could support ultraviolet polarisation vision. R8 cells of rows 5 and 6 are known to act as quarter-wave retarders around 500 nm and thus are the first photoreceptor type described with a potential dual role in polarisation vision.

S. Kleinlogel (✉) · N. J. Marshall
Sensory Neurobiology Group, School of Biomedical Sciences,
University of Queensland, Brisbane, QLD 4072, Australia
e-mail: Sonja.Kleinlogel@mpibp-frankfurt.mpg.de

Present Address:
S. Kleinlogel
Max-Planck-Institut für Biophysik,
60438 Frankfurt am Main, Germany

Abbreviations

R-log I function	Intensity response function
ϕ_{max}	*e*-Vector angle eliciting a maximum response
λ_{max}	Peak wavelength of spectral sensitivity function
R1–R8	Retinular cells (photoreceptors) 1 to 8
PS	Polarisation sensitivity
UV	Ultraviolet

Introduction

Stomatopod crustaceans of the species *Odontodactylus scyllarus* live in shallow, clear waters of coral reefs from subtidally down to depths of 30 m (Caldwell and Dingle 1976). They prey on fish and invertebrates, such as snails, crabs and molluscs, which they hit or stab with their two rapidly moving raptorial appendages (Fig. 1a; Caldwell and Dingle 1976). Their aggressive lifestyle requires elaborate visual capabilities. The stalked apposition compound eyes of *Odontodactylus scyllarus*, like those of other gonodactyloid stomatopods, are divided into a dorsal and a ventral hemisphere by an equatorial mid-band of six rows of enlarged ommatidia, numbered 1 to 6 from dorsal to ventral (Fig. 1b, c). Mid-band rows 1–4 are thought to process chromatic signals, whereas mid-band rows 5 and 6 have been implicated in polarisation vision (Marshall 1988; Marshall et al. 1989, 1991; Kleinlogel and Marshall 2006;
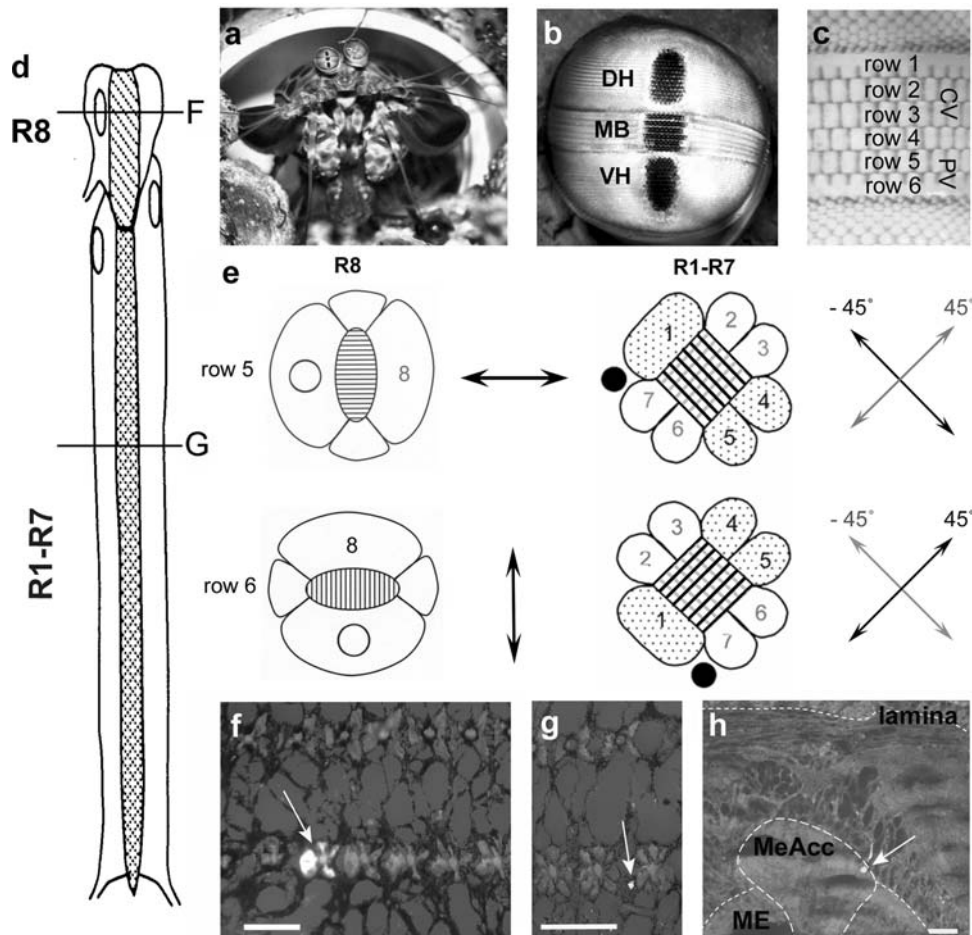
Fig. 1 The visual system of *Odontodactylus scyllarus*. **a** *Odonto-dactylus scyllarus* photographed in one of our marine aquaria. Notice the folded raptorial appendages and the large, independently moving eyes. **b** Close-up view of a single eye. The eye is divided into a dorsal (*DH*) and a ventral hemisphere (*VH*) by a six-rowed mid-band (*MB*) of enlarged ommatidia. The three dark pseudopupils reveal the overlapping visual fields of the three eye regions. **c** Photomicrograph of the mid-band region of the cornea, which consists of 6 rows, numbered rows 1 to 6 from dorsal to ventral. Rows 1–4 are implicated with colour vision (*CV*) and rows 5 and 6 with polarisation vision (*PV*). **d** Diagram of a longitudinal section through a mid-band rows 5 and 6 ommatidium, which is composed of a distally placed small retinal cell, the R8 cell, and a longer fused main rhabdom constructed from seven retinular cells, the R1–R7 cells. Ultraviolet linear polarisation vision is mediated by the distal R8 photoreceptors. The R8 cell body is four-lobed with the nucleus positioned in the biggest lobe above photoreceptors R1 and R7; from this lobe the axon originates and projects proximally to R1 and R7 to the basement membrane of the retina. **e** Diagrams of the photoreceptor arrangements within mid-band row 5 (*top*) and mid-band row 6 (*bottom*) in

frontal view. The diagrams on the left show sections at the level of the R8 cells and the diagrams on the right show sections at the level of the R1–R7 cells. Note that the cell arrangement in row 6 is rotated 90° counter-clockwise compared to row 5 as identified by the R8 nucleus (*open circle*) and the R8 axon position (*black circle*). The *arrows* next to the diagrams indicate the microvillar orientations of photoreceptors. Mid-band row 5 R8 cells produce microvilli oriented at 90° (*horizontal*) and mid-band row 6 R8 cells produce microvilli oriented at 0° (*vertical*). The R1–R7 cells (numbered *1–7*) form two cell groups (R1, R4, R5 stippled/R2, R3, R6, R7 plain) with microvilli at 45° and −45° and are sensitive to orthogonal *e*-vector directions. See Marshall et al. (1991) for anatomical details. **f–h** Three photomicrographs from series of 7-μm thick frontal sections through the eye show a Lucifer yellow filled R8 cell of mid-band row 5 (*arrows*) at the levels of (**f**) its cell body in the distal retina, (**g**) its axon projecting alongside photoreceptor R7 and (**h**) its terminal in the distal accessory lobe of the medulla externa (MEAcc). The levels at which sections (**f**) and (**g**) were taken are indicated in (**d**). *Scale bars* 50 μm

Marshall et al. 2007). The fused rhabdoms of mid-band rows 5 and 6 are based on a two-tiered design, typical of many crustaceans (Fig. 1d). The main rhabdom is formed by seven retinular cells, R1 to R7, overlayed by a much smaller, four-lobed retinular cell, the R8 cell (Marshall et al. 1991).

The R1–R7 cells typically mediate polarisation sensitivity in crustaceans. These cells form two groups, which produce orthogonal layers of microvilli throughout the rhabdom and therefore can be compared to analyse environmental polarised light (Fig. 1e; Eguchi and Waterman 1966; Waterman 1981; Sabra and Glantz 1985; Marshall

et al. 1991; Kleinlogel and Marshall 2006). Although R1–R7 cells signal polarisation in the middle-wavelength region around 500 nm, polarisation sensitivity to shorter wavelengths is also found in crustaceans (Waterman and Fernandez 1970). The R8 cells of investigated gonodactyloid stomatopod species are sensitive to ultraviolet light (Cronin et al. 1994; Marshall and Oberwinkler 1999). While the majority of R8 cells in gonodactyloid stomatopods form microvilli that are arranged orthogonally, and are thus most likely insensitive to polarised light, R8 cells in mid-band rows 5 and 6 produce unidirectional microvilli. Their rhabdomeres are also significantly longer than the rhabdomeres of R8 cells in the remainder of the retina, in *Odontodactylus scyllarus* for example, they are 150 μm long while the R8 cells of the other mid-band rows are in average 97 μm long. These two adaptations suggest a possible increase in sensitivity to linearly polarised light (Marshall et al. 1991; Marshall and Oberwinkler 1999). It has previously been demonstrated with non-invasive optical physiology that the R8 cells in the 5th and 6th ommatidial rows of *Neogonodactylus oerstedii* are polarisation-sensitive (Cronin et al. 1994), confirming this idea experimentally. In *Neogonodactylus oerstedii*, *Odontodactylus scyllarus* and other stomatopod species with six row mid-bands, the profile of rows 5 and 6 R8 cells is oval-shaped in transverse section, the microvillar direction being orthogonal to the long axis of the oval (Fig. 1e). It was the orthogonal arrangement of these oval-shapes between rows 5 and 6, where those in row six run parallel to the long-axis of the mid-band and those in row 5 perpendicular to the mid-band, that first suggested polarisation sensitivity in these two rows (Marshall 1988; Marshall et al. 1991; Cronin et al. 1994).

Polarisation vision has been studied most thoroughly in the gonodactyloid species *Odontodactylus scyllarus*. This species possesses sophisticated linear polarisation vision in the middle-wavelength region of the spectrum (Marshall et al. 1999). Certain body parts involved in signalling behaviours reflect linearly polarised light and may be used in communication (Chiou et al. 2005). But most strikingly, *Odontodactylus scyllarus*' photoreceptors R1–R7 in mid-band rows 5 and 6 are sensitive to circular polarised light (Chiou et al. 2008; Kleinlogel and White 2008). The ability to detect circular polarised light with linear polarisation detectors is mediated by the overlying R8 cells, which act as quarter-wave retarders around 500 nm and convert incoming circular polarised light to linear polarised (Chiou et al. 2008; Roberts et al. 2009). Knowing this, the immediate question is whether the R8 cells of *Odontodactylus scyllarus* can simultaneously detect ultraviolet linear polarised light? This would mean that they have two different roles, one for enabling circular polarisation detection near 500 nm and one for UV linear polarisation

detection. Such a dual role photoreceptor has never been described before.

To investigate this, we set out to examine the polarisation and spectral characteristics of R8 cells in the mid-band of *Odontodactylus scyllarus*. Light-evoked responses were recorded using intracellular electrodes and physiologically characterised cells subsequently labelled with fluorescent dyes. Indeed, R8 cells in rows 5 and 6 responded strongly to linear polarised UV light with an *e*-vector aligned parallel to their microvillar axes: the R8 cells in row 5 were most sensitive to light with an *e*-vector oriented parallel to the mid-band, whereas row 6 R8 cells were most sensitive to light with an *e*-vector oriented perpendicular to the mid-band. Cells in mid-band rows 1–4 did not show linear polarisation sensitivity as predicted from anatomical observations (Marshall et al. 1991). The spectral sensitivity functions of both, rows 5 and 6 R8 cells, peaked in the ultraviolet at 335 nm, 5 nm shorter to those of *Neogonodactylus oerstedii* (Marshall and Oberwinkler 1999).

Methods

Animals and preparation

As much as 13 adult male and female stomatopods of the species *Odontodactylus scyllarus* (*Linnaeus 1758*, Crustacea, Hoplocarida, Stomatopoda, Gonodactyloidea) were collected by professional collectors (Seafish, Stradbroke Island, Australia; Cairns Marine, Cairns, Australia) and housed under a 12 h:12 h dark/light cycle in marine aquaria approved by the Australian Quarantine Inspection Service (AQIS) and Environment Australia, Wildlife Protection. Animals were anaesthetised by cooling and euthanised by decapitation before the eyes were removed. All procedures were approved by the Animal Ethics Committee (UAEC, per*mit # VTHRC/488/06*) of the University of Queensland.

The amputated eye was mounted on a plastic rod with the help of a low-melting point bee's wax/dental wax mixture (Fig. 2). For this the plastic rod was clamped into a metal block and an attached pin that could be moved along the dorsal–ventral axis of the eye was used for exact alignment of the lateral mid-band with the axis of the rod (Fig. 2a). With the rod in a horizontal position a small hole about 10–20 facets was then cut at the edge of the retina into the lateral dorsal hemisphere with a razor blade. The rod was inserted into a glass bubble filled with oxygenated HEPES buffered stomatopod saline (Fig. 2b) and the glass bubble was positioned at the centre of a Cardan arm perimeter device (Kleinlogel and Marshall 2006). All of the above procedures were performed under red light illumination in order not to bleach the retina.
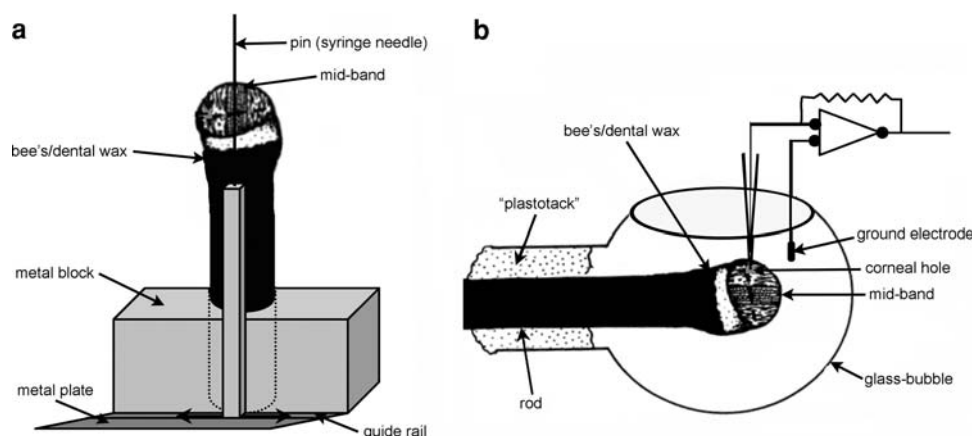
Fig. 2 Eye preparation under red light illumination. **a** A plastic rod was clamped into a metal block and the amputated eye was mounted on the tip of the rod with the help of low-melting point wax. A pin (syringe needle) attached to the metal block that could be moved along the dorsal–ventral axis of the eye via a guide rail was used for exact alignment of the lateral mid-band with the axis of the rod. **b** The eye with the lateral mid-band oriented horizontally was then placed into a glass bubble filled with oxygenated saline and an intracellular electrode was lowered through a small corneal hole cut into the lateral part of the dorsal hemisphere (after Kleinlogel and Marshall 2006)

The light source was a 150 W Xenon-arc lamp (Oriel, Stratford, USA) in combination with a computer-controlled monochromator (Model 77200; Oriel, Stratford, USA). For spectral measurements, a monochromator slit-width of 1.24 mm was used, which produced light of a spectral composition of approximately 8 nm bandwidth. For polarisation measurements, light with a 20 nm bandwidth was used. The light beam was first passed through a circular, computer-controlled neutral density wedge (50 mm, ND 0-4, Model 7230, Optique Instrumental MTO, Massy, France) and an electronic shutter (Uniblitz, Model LS6T2, New York, USA). The neutral density wedge was programmed to produce equal quantal fluxes at each wavelength during spectral scan measurements and allowed for intensity variations of 4 log units (OD 0.04-4) during monochromatic polarisation measurements. The light was then focussed into a flexible ultraviolet-transmitting liquid (water) light-guide (Edmund Optics, Model NT53-691, York, UK) that was attached to the perimeter device, where it provided a point source of light of 0.9° visual angle. To determine the linear polarisation sensitivity, an ultraviolet-transmitting linear polarisation filter (Polaroid HNP'B, effective in both visible and ultraviolet spectral regions) was inserted between the tip of the light guide and the eye, the angle of which could be changed in steps of 10° relative to the eye. To test the consistency of polarised light transmission through the entire optical system with wavelength and polariser angle, we measured the relative photon flux at the position of the eye with an USB 2000 spectrometer (Ocean Optics, Dunedin, Florida, USA) calibrated against a secondary NIST standard lamp (Oriel, Stratford, USA) using OOIBase32 software (Ocean Optics, Dunedin, Florida, USA). The transmitted light intensity was determined at each wavelength from 299 nm to 750 nm for every 10° of polariser angle. We corrected electrophysiological polarisation raw data from photoreceptors in order to compensate for the system's polarisation transmission irregularities, which showed that the introduced response artefacts lie within the noise level of electrophysiological recordings (~ 1 mV) and are thus negligible.

Intracellular recordings

Microelectrodes filled with either 1% ethidium bromide (Sigma–Aldrich, USA) in 1 M KCl (40–100 MΩ) or 5% Lucifer yellow CH (Sigma–Aldrich, Australia) in 1 M LiCl (100–250 MΩ) were lowered vertically into the retina through the corneal hole cut into the dorsal lateral hemisphere. The pipette was connected to the headstage of an intracellular amplifier (Axoprobe 1A, Axon Instruments, Union City, CA, USA) via a chlorided silver electrode. An Ag/AgCl pellet immersed in saline served as a ground electrode (Fig. 2). When a stable recording was achieved, the stimulus position was adjusted for maximal light response in 1° angular steps in the vertical and horizontal axes to ensure alignment of the light source with the visual axis of the photoreceptor. Only photoreceptors with a resting membrane potential of about −60 mV and a response to a brief test flash of white light (the grating of the monochromator was bypassed by a surface-mirror) of 30 mV or more were subjected to further analysis.

The photoreceptor was first characterised by its spectral sensitivity, which was measured with the spectral scan method (Menzel et al. 1986; Kleinlogel and Marshall 2006). To determine the linear polarisation sensitivity, the angle of the polarisation filter was changed in angular steps of 10° or 20° relative to the eye (0° = vertical e-vector direction, orthogonal to the mid-band) whilst the eye was stimulated

with brief (50 ms) flashes of light (*e*-vector angle vs. response amplitude curves). Polarisation sensitivity measurements were performed at the peak wavelength of the spectral sensitivity function of the photoreceptor. Two peak response versus relative light intensity (*R*-log I) functions were then recorded at the maximum (ϕ_{max}) and minimum (ϕ_{min}) response angles, respectively. Single photoreceptor responses were digitised on a virtual oscilloscope (ADC-100) using PicoScope software (Pico Technology, Camperdown, NSW, Australia) and then exported into Microsoft Excel for analysis. At the end of each recording, cells were iontophoretically labelled either with Lucifer yellow, using hyperpolarising current pulses (−1 nA; 1 Hz; 50% duty cycle) for 5 min, or with ethidium bromide, using depolarising current pulses (1 nA; 1 Hz; 50% duty cycle) for 4 min. The eyes were then fixed in 4% paraformaldehyde and embedded in 2-hydroxyethylmethacrylate (Technovit T7100, Heraeus, Germany). Unstained transverse sections of 7 μm thickness were observed and photographed with a Zeiss Axioscope microscope (10×/0.30 and 20×/0.5 objectives) equipped with a digital SPOT camera (Diagnostic Instruments, Sterling Heights, MI, USA) using fluorescent microscopy and ALPHA Vivid standard Lucifer yellow XF14 filters (Omega Optical, Inc., Brattleboro, VT, USA). Contrast was enhanced using Adobe Photoshop 7.0 (Adobe Systems). Labelled R8 receptors and their projections were traced from their cell bodies in the distal retina to their terminals in the distal medulla externa (Fig. 1f–h).

Data analysis

Datasets were only accepted if there were no appreciable changes in resting membrane voltage or in maximal response amplitudes during the experiment. Since the principle of univariance applies, we used only polarisation datasets with consistent ϕ_{max} and ϕ_{min} and approximately parallel *R*-log I curves for further analysis (Naka and Rushton 1966; Laughlin 1975).

R-log I curves were fitted with a hyperbolic tangent (Naka–Rushton) function (Naka 1969) using least-squares approximation in Origin 6.1 (OriginLab Corporation, Northampton, MA, USA). Polarisation sensitivity (PS) was computed from the log-intensity shift (δi) between the fitted *R*-log I curves, with *i* being the relative intensity at half-saturation, determined from the fitted Naka–Rushton curves (Fig. 4c, d):

$$PS = 10^{\delta i}$$

For cells with equal sensitivity to any *e*-vector direction PS = 1 since $\delta i = 0$.

The *e*-vector angle versus response amplitude curves from successive recordings on a single cell were averaged and then normalised by setting the maximum amplitude to

1 and the minimum amplitude to 0. The normalised curves were then again averaged over all cells and the resulting response amplitude curve fitted with a function of the form:

$$S = k + w \times \cos(2\phi - 2\phi_{max})$$

where *k* is the shift of the function along the *y*-axis, *w* is the amplitude dependent on the degree of polarisation of the stimulus light and the photoreceptor's polarisation sensitivity, ϕ is the polaroid angle and ϕ_{max} is the polaroid angle that maximises *S* (Bernard and Wehner 1977). This function predicts normalised photon catch as a function of *e*-vector angle. The goodness of fit suggests that, although the photoreceptor response rises non-linearly with photon catch, according to the Naka–Rushton relationship, the photoreceptors were operating in their quasi-linear range.

Terminology

To simplify the description of the eye's anatomy, the text and all subsequent figures describe the directions as seen in a frontal view of a right eye with the mid-band oriented horizontally. In a left eye, the photoreceptor arrangement is mirror-symmetric. Angles are given relative to the zero-position of the polariser, so that 0° is the *e*-vector orientation perpendicular to the mid-band.

Results

Since this study aimed to investigate the polarisation sensitivities of mid-band rows 5 and 6 R8 cells, our main effort was to record within this structurally specialised region. Recordings from R8 cells encountered outside mid-band rows 5 and 6 were also examined; these photoreceptors produce perpendicular sets of microvilli and are therefore expected to have equal sensitivity to any *e*-vector orientation of light (Marshall et al. 1991). Recordings were made from eight mid-band rows 5 and 6 R8 cells and 19 R8 cells located outside this specialised region in 24 eyes of female and male stomatopods of the species *Odontodactylus scyllarus*. Each cell was tested for its polarisation and spectral sensitivities and subsequently labelled for identification. No noticeable discrepancies were found between male and female stomatopods.

Linear polarised light sensitive R8 cells

Five row 5 R8 cells and three row 6 R8 cells were successfully labelled with fluorescent dyes and analysed (Figs. 1f–h, 3e). Mid-band rows 5 and 6 R8 cells possessed identical spectral sensitivity functions, with a maximum at 335 ± 7.2 nm (mean ± S.D., *n* = 8) and a halfwidth of 46 ± 7.1 nm (mean ± S.D., *n* = 8), with no measurable
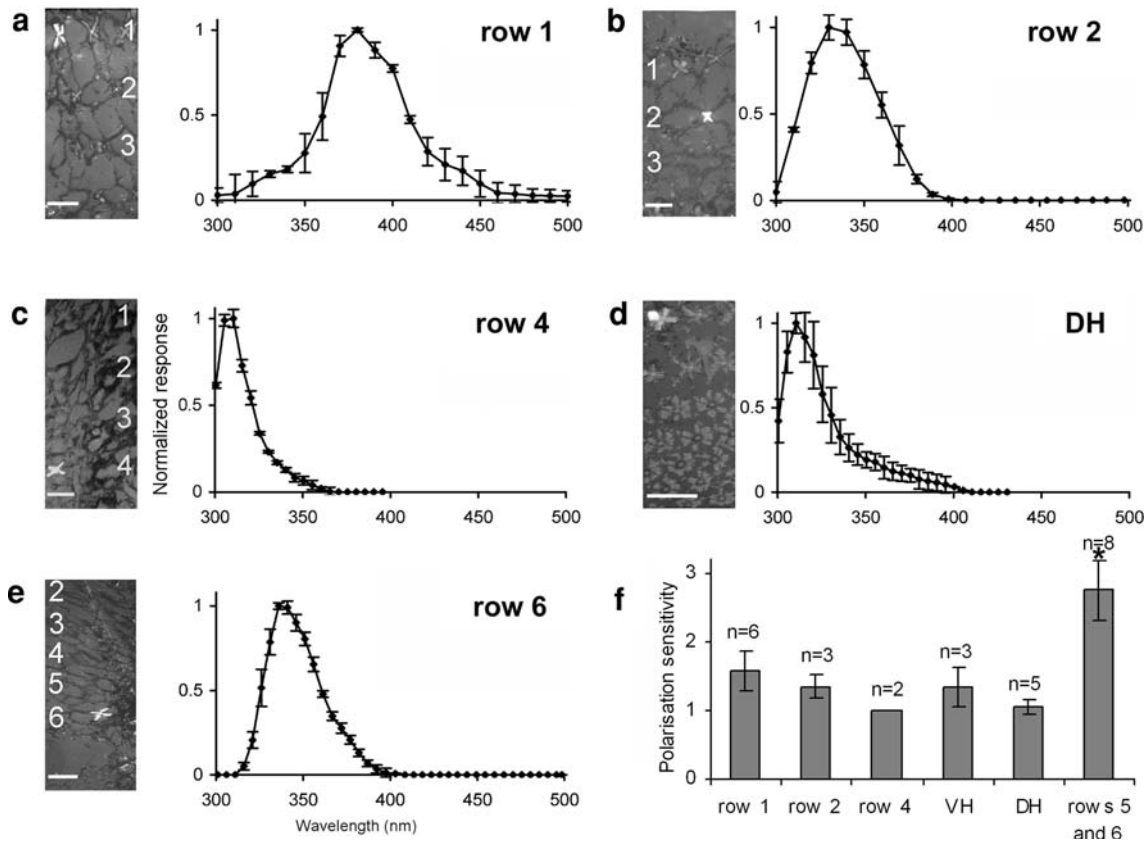
Fig. 3 Anatomical groups of R8 cell types within the stomatopod retina. **a–e** Each panel shows a fluorescence micrograph of a frontal retinal section (similar Fig. 1f; mid-band rows 1–6 numbered) containing a dye-labelled R8 cell on the left and an averaged, normalised spectral sensitivity functions (mean ± S.D.; data points connected with lines) on the right. *Scale bars* 50 μm. The determined peak sensitivities (mean ± S.D.) are **a** 381 ± 6 nm ($n = 6$) for mid-band row 1 R8 cells, **b** 330 ± 7 nm ($n = 3$) for mid-band row 2 R8 cells, **c** 311 ± 3 nm ($n = 2$) for mid-band row 4 R8 cells, **d** 311 ± 14 nm ($n = 8$) for hemispheric R8 cells and **e** 335 ± 7.2 nm ($n = 8$) for mid-band rows 5 and 6 R8 cells. **f** Polarisation sensitivities (values are mean ± S.D.). The mean PS value of mid-band rows 5 and 6 R8 cells is significantly higher than the PS values of R8 cells outside this specialised area. *VH* ventral hemisphere, *DH* dorsal hemisphere

sensitivity to wavelengths beyond 400 nm (Fig. 3e). All photoreceptors anatomically assigned to mid-band rows 5 and 6 were sensitive to linearly polarised ultraviolet light with an average PS value of 2.75 ± 0.42 (mean ± S.D., $n = 8$; Fig. 4a–c). Row 5 R8 cells had a ϕ_{max} oriented parallel to the mid-band at $86.83° \pm 6.86°$ (mean ± S.D., $n = 5$), whereas the ϕ_{max} of row 6 R8 cells was oriented vertical to the mid-band at $-1.63° \pm 1.36°$ (mean ± S.D., $n = 3$). The orthogonal arrangement of the ϕ_{max}s of rows 5 and 6 R8 cells conforms with the 90° counter-clockwise rotation of the photoreceptor arrangement in row 6 ommatidia compared to row 5 ommatidia (see Fig. 1e; Marshall et al. 1991).

R8 cells located outside mid-band rows 5 and 6

We successfully labelled and analysed 19 R8 cells located outside mid-band rows 5 and 6. The cells could be categorised into four anatomical groups according to their location in the retina. Six cells were located in mid-band

row 1. Their spectral sensitivity function had a maximum (λ_{max}) at 381 ± 6 nm (mean ± S.D.) and a halfwidth of 50 ± 5.0 nm (mean ± S.D., Fig. 3a). Their averaged polarisation sensitivity was 1.57 ± 0.29 (mean ± S.D., Fig. 3f). Three cells were located in mid-band row 2. Their spectral sensitivity function had a λ_{max} at 330 ± 7 nm (mean ± S.D.) and a halfwidth of 51 ± 4.0 nm (mean ± S.D.) and their averaged polarisation sensitivity was 1.35 ± 0.17 (mean ± S.D., Figs. 3b, f, 4d). Two cells were located in mid-band row 4. Their spectral sensitivity function had a λ_{max} at 311 ± 3 nm (mean ± S.D.) and a halfwidth of 25 ± 1.0 nm (mean ± S.D.) and their averaged polarisation sensitivity was 1.0 ± 0.0 (mean ± S.D., Fig. 3c, f). Dorsal and ventral hemispheric R8 receptors had identical spectral sensitivity functions with a λ_{max} of 311 ± 14 nm (mean ± S.D., $n = 8$) and a halfwidth of 24 ± 1.06 nm (Fig. 3d). Their averaged polarisation sensitivity was 1.16 ± 0.23 (mean ± S.D., $n = 8$). Three cells were located in the ventral hemisphere with a
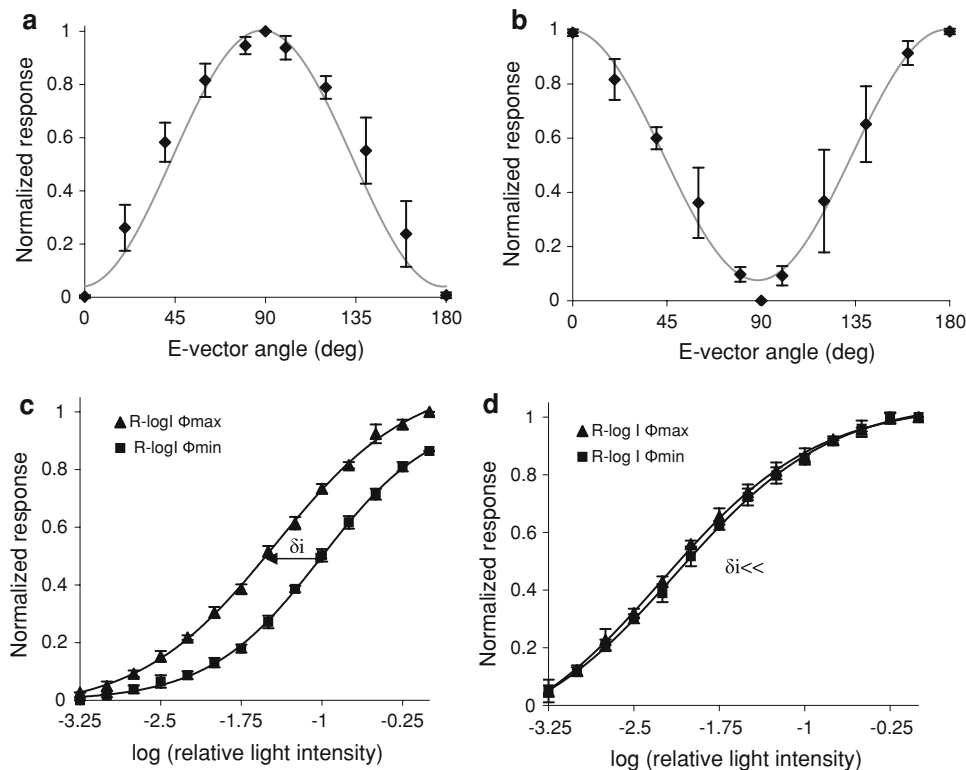
Fig. 4 Electrophysiological recordings from linear polarisation-sensitive R8 cells located within and outside mid-band rows 5 and 6. **a, b** Normalised *e*-vector angle versus response amplitude curves from R8 cells in **a** mid-band row 5 ($n = 5$) and **b** mid-band row 6 $n = 3$, fitted to a predicted functional response curve (*smooth lines*). Mid-band row 5 R8 cells have a ϕ_{max} at $86.83° \pm 6.86°$ (mean $\pm$ S.D.) and row 6 R8 cells at $-1.63° \pm 1.36°$. **c, d** Peak response versus relative light intensity for (**c**) a row 6 R8 cell and (**d**) a row 2 R8 cell. *Top curves* are measured at the maximum response anlge, ϕ_{max}, and bottom curves at ϕ_{min} (mean $\pm$ S.D., two runs each). The *smooth lines* are sigmoidal curves fitted to a hyperbolic tangent function. The polarisation sensitivity, $10^{\delta i}$, is measured by taking the difference between intensities at half-maximal response, δi. **c** $10^{\delta i} = 3.33$, the highest polarisation sensitivity value measured for a mid-band row 6 R8 cell; **d** $10^{\delta i} = 1.15$, representing the negligible polarisation sensitivities of R8 cells in the remainder of the retina

polarisation sensitivity of 1.33 ± 0.29 and five cells were located in the dorsal hemisphere with a polarisation sensitivity of 1.06 ± 0.11 (Fig. 3f; mean $\pm$ S.D., $n = 5$).

No mid-band row 3 R8 cell was successfully labelled; however, the possible identity of unlabelled photoreceptors can be inferred from the depth of the recording electrode and the measured spectral sensitivity function. From this, putative row 3 R8 receptors had no sensitivity to linear polarised light. However, unlabelled cells were not included in the analysis.

In summary, R8 cells from mid-band rows 5 and 6 had significantly higher polarisation sensitivity values than other R8 cells (Fig. 3f); this also holds for mid-band row 1 R8 cells with the highest polarisation sensitivities (student's *t* test, $p < 0.0002$).

Discussion

We were able to demonstrate sensitivity to linear polarised ultraviolet light selectively for R8 cells located within mid-band rows 5 and 6. This is consistent with predictions from the anatomy of these cells, as is the very low polarisation sensitivity in the rows 1–4 R8 cells, these cells possessing bidirectional microvilli in the same cell (Marshall et al. 1991). The fact that there is any polarisation sensitivity at all in these cells suggests a possible slight imbalance in the number of microvilli in each direction or alternatively physiological or other structural differences that are not clear. Also it is not clear whether this small PS value would confer any advantage. The measured linear polarisation sensitivity values of 2.75 ± 0.42 (mean $\pm$ S.D., $n = 8$) are consistent with the PS values determined using the pupillary responses of *Neogonodactylus oerstedii* (3.01 ± 1.06; Cronin et al. 1994). Intracellular recordings from the violet-sensitive cells—thought to be R8s—of the crayfish *Procambarus* gave similar PS values (Waterman and Fernandez 1970).

R8 cell mediated polarisation vision

Most crustaceans possess only one class of short-wavelength sensitive R8 cells, which may function as polarisation analysers in some species (Waterman 1981). While a

single polarisation analyser channel may be useful for a number of purposes, such as communication or increasing contrast (Schechner et al. 2003; Chiou et al. 2005), it can only provide information about polarisation properties of a stimulus if it is rotated and the signal examined temporally. If the eye does not rotate, polarisation analysis for many tasks requires at least two input channels, with different e-vector sensitivities (Bernard and Wehner 1977). Stomatopods are the only crustaceans known to possess two classes of polarisation-sensitive R8 cells: the R8 cells of mid-band row 5 are sensitive to horizontal e-vector orientations and the R8 cells of mid-band row 6 are sensitive to vertical e-vector orientations, when the eye is held with the mid-band horizontal. Orthogonality between the two rows is achieved by a 90° counter-clockwise rotation of row 6 ommatidia relative to row 5 ommatidia (see Fig. 1e; Marshall et al. 1991). It is therefore tempting to speculate that these orthogonal UV sensitive R8 channels may be compared antagonistically, as it is common with the two orthogonal input channels from the 500 nm sensitive R1–R7 cells in other crustacean systems (Sabra and Glantz 1985; Glantz 2001; Kleinlogel and Marshall 2006). This requires cross talk between the two sets of R8 cells (between rows) and so far a little evidence exists for this (Kleinlogel and Marshall 2005). Such an opponent ultraviolet system between mid-band rows 5 and 6 would explain why there are two otherwise structurally and functionally identical rows within the mid-band, but rotated relative to each other at 90°.

Two-channel polarisation vision may be insufficient for some tasks since such systems have inherent confusion points at ±45° from the orthogonal directions (Bernard and Wehner 1977). Odontodactylus scyllarus and other stomatopods may overcome this restriction through their unusual ability to rotate the eye about the eye-stalk axis, adding a third, temporal dimension to the 'static' polarisation-sensitive system (Land et al. 1990). Thus, Odontodactylus scyllarus may possess temporally tunable or optimised linear polarisation vision in the ultraviolet spectrum, a feature currently used in underwater scatter-reduction technologies (Schechner and Karpel 2004).

It is remarkable that linear UV polarisation sensitivity is not the only function of mid-band rows 5 and 6 R8 cells in polarisation vision. They also mediate one-fourth wave retardance, with an astonishingly flat spectral response and are a vital optical component in the circular polarisation sensitivity system of the rows 5 and 6 R1–R7 cells (Chiou et al. 2008). The R8 cells convert incoming visible circularly polarised light to linearly polarised light, which is then detected by the alternating stacks of microvilli produced by R1–R7 (Chiou et al. 2008; Kleinlogel and White 2008). This is the only known example of a dual role in polarisation vision of a single photoreceptor type, separated

solely by the spectrum of action; linear polarisation vision in the UV and one-fourth wave retardation allowing circular polarisation detection around 500 nm.

Biological significance of ultraviolet polarisation vision

It is interesting that the UV spectral sensitivities of the R8 cells in Odontodactylus scyllarus are similar to those of Neogonodactylus oerstedii, particularly the very short spectral sensitivity in the UVb between 310 and 320 nm in mid-band row 4, as the habitat of Odontodactylus scyllarus is, on average, deeper than that of Neogonodactylus oerstedii, and the increased attenuation of UV in deeper water would constrain the spectral sensitivities to longer wavelengths (Caldwell and Dingle 1976; Cronin et al. 1994; Marshall and Oberwinkler 1999). Odontodactylus scyllarus is, however, also found in the top 1–2 m of water, as is Neogonodactylus oerstedii, possibly explaining this 'depth' of UV sensitivity in these individuals. It remains for future work to determine if the UV spectral sensitivity set of stomatopods is tuned to environmental habitat as the red end of their spectral range is (Cronin et al. 1991).

Stomatopods are the only marine animals known with specialised ultraviolet polarisation vision, although we do not know if they actually analyse ultraviolet polarisation or if they just see a contrast signal. This question can only be answered by behavioural experiments. In the following we will discuss possible functions of ultraviolet polarisation vision of Odontodactylus scyllarus.

A few aquatic animals, including crustaceans, equipped with short-wavelength polarisation-sensitive photoreceptors are known to use the celestial polarisation as a compass for orientation (Waterman 1974; Goddard and Forward 1991; Hawryshyn 1992; Schwind 1999; Hawryshyn 2000). Whether still coherent UV polarised light from the sky reaches all depths inhabited by Odontodactylus scyllarus is unknown, but in still waters is theoretically possible (Horváth and Varjú 1995; Frank and Widder 1996). The animals used in our study were mostly collected from shallow and clear water around coral reefs, at depths ranging from subtidal to ∼10 m. In clear water the atmospheric ultraviolet polarisation pattern is fully visible to depths of 2–3 m, but both, waves and in water scatter would rapidly degrade the polarisation signal from the sky at greater depth (Waterman 1954). However, the overall e-vector orientation and degree of polarisation in water are similar from 360 to 550 nm, and the best signal-to-noise ratios will exist at wavelengths at which light is brightest; this is in very shallow water in the ultraviolet and in deep water in the blue (Cronin and Shashar 2001). Maybe for this reason the two sets of photoreceptors in gonodactyloid stomatopods are highly conserved spectrally to two narrow ranges, one near 340 nm and the other near 500 nm.

Other functions for polarisation vision include object detection against scattered light. Reef fish, for example, are opaque and therefore stand out against the strongly scattered and bright ultraviolet background when viewed by an observer with ultraviolet vision (Cronin et al. 1994). Ultraviolet contrast enhancement is less useful when the object reflects light, such as a silvery fish. However, since the reflected light may be polarised differently than the background light, silvery fish may be spotted by an observer with sensitivity to polarised light (Denton and Nicol 1965; Shashar et al. 2000). In fact, any depolarising or birefringent object, which changes the polarisation state of light passing through or reflected from it, can in principle be detected by animals with sufficiently sensitive polarisation vision (Shashar et al. 1998; Sabbah and Shashar 2005). Since polarisation contrast is occasionally maximal in the ultraviolet, a combination of linear polarisation sensitivity with ultraviolet sensitivity may be useful in breaking camouflage systems in shallow water.

Finally, stomatopods have been shown to use controlled reflection of polarised light from certain body parts in conspecific signalling (Cronin et al. 2003; Chiou et al. 2005, 2008). Some of these reflectors show a sufficient degree of polarisation of 20%–50% in the UV (350 nm; Chiou et al. 2005) to be easily detectable by the rows 5 and 6 R8 cells. It remains to be seen if this potential channel for private communication, both in UV and polarisation, has driven the evolution of these photoreceptors.

In conclusion, the polarisation vision system of *Odontodactylus scyllarus* may have evolved to operate in several distinct spectral bands to cope with the large spectral shifts in ambient light encountered in the range of marine environments that it inhabits. The R8 mediated ultraviolet polarisation vision system is specialised for polarisation vision in the bright, ultraviolet-flooded surface waters (Jerlov 1976; Smith and Baker 1981; Frank and Widder 1996; Vasilkov et al. 2005). On the other hand, the middle-wavelengths polarisation receptors (R1–R7) of the hemispheres and mid-band rows 5 and 6 combine linear and circular polarisation sensitivity, providing optimal contrast-enhancement and precise determination of polarisation with no confusion states or neutral points at all depths (Kleinlogel and White 2008). This renders polarisation vision independent of strongly, linearly or circularly polarised features in the animal's environment.

References

Bernard GD, Wehner R (1977) Functional similarities between polarization vision and color vision. Vis Res 17:1019–1028

Caldwell RL, Dingle H (1976) Stomatopods. Sci Am 234:80–89

Chiou TH, Cronin TW, Caldwell RL, Marshall J (2005) Biological polarized light reflectors in stomatopods. SPIE 5888:1–9

Chiou TH, Kleinlogel S, Cronin T, Caldwell R, Loeffler B, Siddiqi A, Goldizen A, Marshall J (2008) Circular polarization vision in a stomatopod crustacean. Curr Biol 18:429–434

Cronin TW, Shashar N (2001) The linearly polarized light field in clear, tropical marine waters: spatial and temporal variation of light intensity, degree of polarization and e-vector angle. J Exp Biol 204:2461–2467

Cronin T, Marshall N, Land M (1991) Optokinesis in gonodactyloid mantis shrimps (Crustacea; Stomatopoda; Gonodactylidae). J Comp Physiol A 168:233–240

Cronin TW, Marshall NJ, Quinn CA, King CA (1994) Ultraviolet photoreception in mantis shrimp. Vis Res 34:1443–1449

Cronin TW, Shashar RL, Caldwell RL, Marshall N, Cheroske AG, Chiou T (2003) Polarization vision and its role in biological signaling. Integr Comp Biol 43:549–558

Denton EJ, Nicol JAC (1965) Studies on reflexions of light from silvery surfaces of fishes, with special reference to the bleak, *Alburnus alburnus*. J Mar Biol Assoc UK 45:683–703

Eguchi E, Waterman TH (1966) Fine structure patterns in crustacean rhabdoms. In: Bernhard CG (ed) The functional organization of the compound eye. Pergamon Press, Oxford, pp 105–124

Frank MT, Widder E (1996) UV light in the deep-sea: in situ measurements of downwelling irradiance in relation to the visual threshold sensitivities of UV-sensitive crustaceans. Mar Behav Physiol 27:189–197

Glantz MR (2001) Polarization analysis in the crayfish visual system. J Exp Biol 204:2383–2390

Goddard SM, Forward RB (1991) The role of the underwater polarized light pattern, in sun compass navigation of the grass shrimp, *Palaemonetes vulgaris*. J Comp Physiol A 169:479–491

Hawryshyn CW (1992) Polarization vision in fish. Am Sci 80:164–175

Hawryshyn CW (2000) Ultraviolet polarization vision in fishes; potential mechanisms for coding e-vector. Philos Trans R Soc Lond B 355:1187–1190

Horváth G, Varjú D (1995) Underwater refraction-polarization patterns of skylight perceived by aquatic animals through Snell's window of the flat water surface. Vis Res 35:1651–1666

Jerlov NG (1976) Marine optics. Elsevier, Amsterdam

Kleinlogel S, Marshall N (2005) Photoreceptor projection and termination pattern in the lamina of gonodactyloid stomatopods (mantis shrimp). Cell Tissue Res 321:273–284

Kleinlogel S, Marshall N (2006) Electrophysiological evidence for linear polarization sensitivity in the compound eyes of the stomatopod crustacean *Gonodactylus chiragra*. J Exp Biol 209:4262–4272

Kleinlogel S, White A (2008) The secret world of shirmps: polarisation vision at its best. PLoS ONE 3:1–8

Land MF, Marshall NJ, Brownless D, Cronin TW (1990) The eye-movements of the mantis shrimp *Odontodactylus scyllarus* (Crustacea: Stomatopoda). J Comp Physiol A 167:155–166

Laughlin SB (1975) Receptor function in the apposition eye—an electrophysiological approach. In: Snyder AW, Menzel R (eds) Photoreceptor optics. Springer, Berlin, Heidelberg, New York, pp 479–498

Marshall NJ (1988) A unique colour and polarization vision system in mantis shrimps. Nature 333:557–560

Marshall NJ, Oberwinkler J (1999) The colourful world of the mantis shrimp. Nature 401:873–874

Marshall NJ, Land MF, Cronin TW (1989) The structure and function of the mid-band in the eyes of stomatopod crustaceans. J Mar Biol Assoc UK 69:735

Marshall NJ, Land MF, King CA, Cronin TW (1991) The compound eyes of mantis shrimps (Crustacea, Hoplocarida, Stomatopoda). I. Compound eye structure: the detection of polarised light. Phil Trans R Soc Lond B 334:33–56

Marshall NJ, Cronin TW, Shashar N, Land M (1999) Behavioural evidence for polarisation vision in stomatopods reveals a potential channel for communication. Curr Biol 9:755–758

Marshall J, Cronin T, Kleinlogel S (2007) Somatopod eye structure and function: a review. Arthropod Struct Dev 36:420–448

Menzel R, Ventura DF, Hertel H, de Souza JM, Greggers U (1986) Spectral sensitivity of photoreceptors in insect compound eyes: comparison of species and methods. J Comp Physiol A 158:165–177

Naka KI (1969) Computer assisted analysis of S-potentials. Biophys J 9:845–859

Naka KI, Rushton WAH (1966) An attempt to analyse colour reception by electrophysiology. J Physiol Lond 185:555–586

Roberts N, Chiou T-H, Marshall N, Cronin T (2009) A biological quarter-wave retarder with excellent achromaticity in the visible wavelength region. Nat Photonics (Published online)

Sabbah S, Shashar N (2005) Polarization contrast of zooplankton: a model for polarization-based sighting distance. Vis Res 46:444–456

Sabra R, Glantz RM (1985) Polarisation sensitivity of crayfish photoreceptors is correlated with their termination sites in the lamina ganglionaris. J Comp Physiol 156:315–318

Schechner Y, Karpel N (2004) Clear underwater vision. Proc Comput Vis Pattern Recognit 1:536–543

Schechner Y, Narasimhan S, Nayar S (2003) Polarization-based vision through haze. Appl Opt 42:511–525

Schwind R (1999) Daphnia pulex swims towards the most strongly polarized light—a response that leads to 'shore flight'. J Exp Biol 202:3631–3635

Shashar N, Hanlon R, Petz A (1998) Polarization vision helps detect transparent prey. Nature 393:222–223

Shashar N, Hagan R, Boal JG, Hanlon RT (2000) Cuttlefish use polarization sensitivity in predation on silvery fish. Vis Res 40:71–75

Smith RC, Baker KS (1981) Optical properties of the clearest natural waters (200–800 nm). Appl Opt 20:177–184

Vasilkov AP, Herman JR, Ahmad Z, Kahru M, Mitchell BG (2005) Assessment of the ultraviolet radiation field in ocean waters from space-based measurements and full radiative-transfer calculations. Appl Opt 44:2863–2869

Waterman TH (1954) Polarization patterns in submarine illumination. Science 120:927–932

Waterman TH (1974) Underwater light and the orientation of animals. In: Jerlov NG, Steemann Nielsen E (eds) Optical aspects of oceanography. Academic Press, New York, pp 415–441

Waterman TH (1981) Polarisation sensitivity. In: Autrum H (ed) Handbook of sensory physiology. Springer, Berlin, pp 283–469

Waterman TH, Fernandez HR (1970) E-vector and wavelength discrimination by retinular cells of the crayfish Procambarus. Z Vgl Physiol 68:154–174